DUBLIN CITY UNIVERSITY
SCHOOL OF ELECTRONIC ENGINEERING

A Final Project report in

Simulation and exploration of THz TRNASMISSION LINES

By Mohammed AL Shuaili

BACHELOR OF ENGINEERING

IN

ELECTRONIC AND COMPUTER ENGINEERING

MAJORING IN

THE INTERNET OF THINGS

Supervised by Dr Marissa Condon

Acknowledgements

Declaration

I declare that this material, which I now submit for assessment, is entirely my own work and has not been taken from the work of others, save and to the extent that such work has been cited and acknowledged within the text of my work. I understand that plagiarism, collusion, and copying are grave and serious offences in the university and accept the penalties that would be imposed should I engage in plagiarism, collusion or copying. I have read and understood the Assignment Regulations set out in the module documentation. I have identified and included the source of all facts, ideas, opinions, and viewpoints of others in the assignment references. Direct quotations from books, journal articles, internet sources, module text, or any other source whatsoever are acknowledged and the source cited in the assignment references. This assignment, or any part of it, has not been previously submitted by me or any other person for assessment on this or any other course of study.

I have read and understood the DCU Academic Integrity and Plagiarism policy at https://www.dcu.ie/policies/academic-integrity-plagiarism-policy

Name: Mohammed Al Shuaili Date: 21/2/2025

Abstract

This final report presents the simulation and exploration of terahertz (THz) transmission lines, focusing on the development and validation of numerical models for high-frequency applications. The project addresses the challenges of accurately modelling THz transmission lines, which are essential for next-generation technologies such as 6G networks, wireless data centres, and biomedical imaging. The primary goal is to create computationally efficient and precise models capable of simulating time-domain behaviour at THz frequencies. Three key methods were employed: the Finite-Difference Time-Domain (FDTD) approach for initial approximations, the Numerical Inverse Laplace Transform (NILT) for exact s-domain solutions, and RLC ladder approximations for efficient time-domain modelling. The FDTD simulations provided a baseline for understanding transient and steady-state behaviours, while the RLC ladder method, combined with NILT, demonstrated the ability to closely match exact solutions when sufficient sections were used. Additionally, Y-parameters were derived to analyse transmission line behaviour, and Asymptotic Waveform Evaluation (AWE) was implemented to refine approximations and extract dominant system responses. The final model was obtained through iterative addition of small responses at high frequencies and comparison with exact solutions. The results highlight the importance of optimising the number of sections in the model to balance accuracy and computational efficiency. This work contributes to the advancement of THz communication systems by providing reliable modelling tools for future research and development.

Table of Contents

Table of Figures

Chapter 1 – Introduction

The growth of communication technologies has led to the exploration of terahertz (THz) frequencies (0.1 to 10 THz) for applications like 6G networks, wireless data centres, and biomedical imaging, but accurate THz transmission line models remain a challenge. The motivation comes from the demand for high-speed THz communication systems, which are crucial for future technologies, but currently lack reliable and efficient modelling tools.

This project aims to develop and validate efficient numerical models for THz transmission lines to predict signal behaviour and optimize system performance. The study addresses key propagation challenges at THz frequencies, such as high attenuation and dispersion, which are critical for the design of next-generation communication systems. To achieve this, the project evaluates original methods and techniques proposed between 2000 and 2010, assessing their suitability for THz applications. In addition, the research focuses on developing an accurate model using Y-parameters and Asymptotic Waveform Evaluation (AWE). The developed model is then compared with the original methods to determine their effectiveness and limitations at THz frequencies

Three primary methods are employed in this study: Finite-Difference Time-Domain (FDTD) for transient analysis, Numerical Inverse Laplace Transform (NILT) for exact s-domain solution, and RLC ladder approximations for computational efficiency. The FDTD method provides a foundation for simulating time-domain electromagnetic wave propagation, while NILT offers precise frequency-domain insights. The RLC ladder approximations, on the other hand, are used to simplify complex transmission line models, making them computationally tractable for large-scale simulations. These methods are compared against each other and the obtained model using Y-parameters and Asymptotic Waveform Evaluation (AWE) to evaluate their effectiveness for THz applications. Factors affecting their performance, such as the number of sections, computational cost, and accuracy, are analysed to determine the most efficient approach for THz transmission line modelling.

The report includes a literature review, implementation details of these modelling methods, simulation results, challenges faced, and future work plans. By integrating Y-parameters and AWE into the modelling framework, this research aims to establish a validated numerical approach for THz transmission line modelling. The proposed model not only addresses the limitations of earlier methods but also offers a computationally efficient and accurate solution for THz signal analysis. By comparing the developed model with original methods from 2000 to 2010, this study provides valuable insights into the evolution of THz modelling techniques and their applicability to modern communication systems. This research

aims to advance THz communication technologies by designing high-performance systems capable of operating at extreme frequencies.

1.2 Summary

This project develops and validates numerical models for THz transmission lines to optimize system performance and address propagation challenges. Three primary methods—FDTD, NILT (exact solution), and RLC ladder approximations—are evaluated for accuracy, computational efficiency, and effectiveness compared to the obtained model using AWE. MATLAB is used for implementation, but these methods can be applied using any coding language or software.

Chapter 2 - **Technical Background**

Modelling THz (0.1–10 THz) transmission lines require understanding wave propagation, transmission line theory, and numerical methods. At THz frequencies, the behaviour of transmission lines is governed by the Telegrapher's equations (1), which describe the relationship between voltage and current along the line. These equations are derived from Maxwell's equations and are given by:

$$\frac{dv(x,t)}{dx} = -R(x)\, i(x,t) - L(x)\frac{di(x,t)}{dt} \qquad (1)$$
$$\frac{di(x,t)}{dx} = -G(x)\, v(x,t) - C(x)\frac{dv(x,t)}{dt}$$

where $v(x,t)$ and $i(x,t)$ represent the voltage and current at position x and time t, respectively. $R,\ L,\ G,$ and C are the per-unit-length resistance, inductance, conductance, and capacitance of the transmission line. At THz frequencies, these parameters become highly frequency-dependent, making accurate modelling more complex.

2.1 Finite-Difference Time-Domain (FDTD) Method

The FDTD method is a widely used numerical technique for solving electromagnetic problems, particularly in the time domain. It discretizes the transmission line into small segments as in Figure 1, allowing for the simulation of voltage and current over time. The FDTD method is based on approximating the derivatives in the Telegrapher's equations using finite differences [3][5]. In this approach voltages (v_n) are calculated at the ends of each section, while currents (i_n) are computed at the middle of each section as illustrated in Figure 1 and 2. Then, v_n and i_n can be derived as.

$$v_k^{n+1} = v_k^n - \frac{\Delta t}{\Delta x C}\left(i_k^{n+\frac{1}{2}} - i_{k-1}^{n+\frac{1}{2}}\right) \qquad (2)$$

$$i_{k-1}^{n+3/2} = i_k^{n+1/2} - \frac{\Delta t}{\Delta x l}\left(v_{k+1}^{n+1} - v_k^{n+1}\right) \qquad (3)$$

This method provides a foundation for simulating transient and steady-state behaviors of transmission lines, but it can be computationally intensive, especially for long lines or high frequencies.

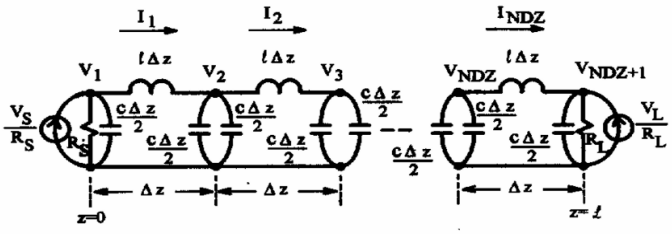

Figure 2: Equivalent representation of the transmission line using the Lumped Pi circuit model, illustrating the discretization of inductance and capacitance along the line [5].

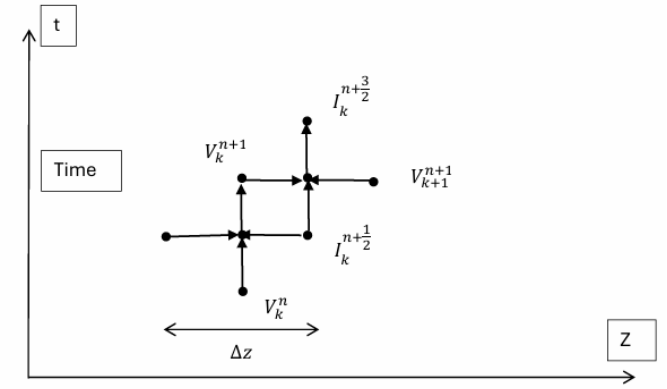

Figure 1: Staggered grid representation for the FDTD method, illustrating the spatial (z) and temporal (t) discretization. The voltage (V) is defined at grid points, while the current (I) is defined at the midpoints between the grid points [5].

2.2 Numerical Inverse Laplace Transform (NILT)

The NILT method is a powerful tool for convert frequency-domain solutions into time-domain solutions for simulating transient phenomena in multiconductor transmission line (MTL) systems [7]. NILT0, the baseline variant, approximates time-domain responses using residues and poles of a Padé rational function, enabling sparse time points with L-stability. NILTn (for $n \geq 1$) extends this by recursively computing high-order derivatives of Laplace-domain solutions, reducing truncation errors by $(n+1)N + M$ while maintaining stability [6]. Furthermore, NILTcv is based on the Bromwich integral, which is numerically evaluated using the Fast Fourier Transform (FFT) and the quotient-difference (q-d) algorithm. The time-domain function $f(t)$ is approximated using a discrete form derived from the Laplace transform $F(s)$ as in (4). The approximation involves a finite sum evaluated by the FFT and an infinite sum accelerated by the q-d algorithm, which uses a continued fraction to improve convergence [7].

$$f(t) = \frac{1}{2\pi j}\int_{c-\infty}^{c+\infty} F(s)e^{st}ds \tag{4}$$

This approach allows for the exact solution of the transmission line's behaviour in the s-domain, which can then be compared with approximate methods such as the RLC ladder to validate accuracy.

2.3 RLC Ladder Approximations

The RLC ladder method approximates a transmission line by dividing it into multiple sections, each represented by lumped resistive (R), inductive (L), and capacitive (C) elements as shown in Figure 3. This discretization simplifies the transmission line into a network of interconnected RLC circuits, making it easier to model and simulate

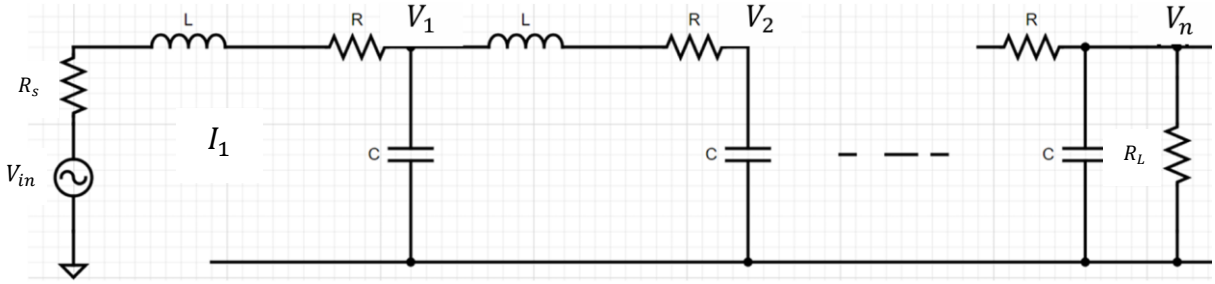

Figure 2.3.1: RLC ladder network approximates a transmission line with N sections and lumped elements (R), (L), and

Governing equations:

Considering one section of the RLC ladder, the following equations are derived:

$$V_s - V_1 = (R + R_s)I_1\, dz + L\frac{dI_1}{dt}dz \tag{5}$$

$$I_1 - I_2 = C\frac{dV_1}{dt}dz \tag{6}$$

Here, dz represents the length of a small segment of the transmission line and is defined as:

$$dz = \frac{l}{N} \tag{7}$$

where l is the total length of the line, and NN is the number of sections or RLC circuits used to model the line.

$$\frac{dI_1}{dt} = -\frac{1}{L}V_1 - \frac{R_s + R}{L}I_1 + \frac{1}{L}V_s \tag{8}$$

$$\frac{dV_1}{dt} = \frac{1}{C}I_1 - \frac{1}{C}I_2 \tag{9}$$

$$\frac{dI_n}{dt} = -\frac{1}{L}V_n - \frac{R_s + R}{L}I_n + \frac{1}{L}V_{n-1} \tag{10}$$

$$\frac{dV_n}{dt} = \frac{1}{C}I_n - \frac{1}{C}I_{n+1} \tag{11}$$

The impedances *R*, *L*, and *C* are defined per unit length (i.e., per *dz*) in Equations (5) and (6). By rearranging Equations (5) and (6), Equations (8) and (9) are obtained. For the *n*-th section, the generalised forms are given by Equations (10) and (11). The accuracy of the RLC ladder approximation depends on the number of sections used; more sections generally lead to higher accuracy but at the cost of increased computational complexity. The RLC ladder method is particularly useful for simulating long transmission lines or systems with complex terminations.

2.4 Asymptotic Waveform Evaluation (AWE):

Asymptotic Waveform Evaluation (AWE) is a computationally efficient technique used to approximate the transient response of large linear systems, such as electrical interconnects, by reducing their high-order state-space models into lower-order approximations. Traditional methods such as SPICE become prohibitively slow for circuits with hundreds of nodes (e.g., PEEC models), but AWE addresses this by extracting dominant poles and residues from the system's transfer function using Padé approximation and moment matching [9]. By focusing on these critical poles, AWE converts the state-space representation—which describes the system's dynamics through differential equations—into a simplified time-domain model.

2.4.1 A general definition of moments in AWE:

The q^{th} moment is defined as:

$$H(s=0) = \int_0^\infty h(t)dt \tag{12}$$

$$H^{(1)}(s=0) = -\int_0^\infty h(t)tdt$$

$$H^{(2)}(s=0) = \int_0^\infty h(t)t^2dt$$

$$H^{(3)}(s=0) = -\int_0^\infty h(t)t^3dt$$

Application of moments to represent the transfer function $H(s)$:

$$H(s) = \int_0^\infty h(t)(1 - st + \frac{1}{2}s^2t^2 - \frac{1}{6}s^3t^3 + \frac{1}{24}s^4t^4dt \tag{13}$$

$$= H(0) + sH^{(1)}(0) + \frac{1}{2}s^2H^{(2)}(0) + \frac{1}{6}s^3H^{(3)}(0) + \cdots$$

$$= m_0 + m_1s + m_2s^2 + m_3s^3 + \cdots$$

$$= \sum_{k=0}^{\infty} \frac{s^k}{k!} H^{(k)}(s=0) = \sum_{k=0}^{\infty} m_k s^k$$

Where

$$m_k = \frac{1}{k!} H^{(k)}(s=0) = \frac{(-1)^q}{q!} \int_0^{\infty} t^q h(t) dt \quad (14)$$

2.5 Y-parameters:

In the analysis of transmission lines, the Y-parameters (admittance parameters) are commonly used to characterize the relationship between the currents and voltages at the input and output ports. These parameters are typically determined experimentally and can be approximated using rational functions of the complex frequency variable (s) as explained in (15) [9].

$$\begin{bmatrix} I_s \\ -I_R \end{bmatrix} = \begin{bmatrix} Y_{11} & Y_{12} \\ Y_{21} & Y_{22} \end{bmatrix} \begin{bmatrix} V_s \\ V_R \end{bmatrix} \quad (15)$$

Each one is approximated with a rational function as in (16):

$$Y_{ij} = \frac{(a_{nij} s^{n-1} + .. + a_{0ij})}{s^n + .. + b_{0ij}} \quad (16)$$

In the open-circuit condition, where the output current (I_R) is zero, the voltage transfer function ($\frac{V_R}{V_s}$) is derived as a ratio of these rational functions (17). This transfer function is then converted into a state-space representation, to facilitate further analysis. Finally, AWE is applied to the state-space model to obtain a time-domain representation, enabling the study of the system's transient and steady-state behavior. This approach provides a systematic method for modeling and simulating the response of transmission lines.

$$\frac{V_R}{V_s} = -\frac{Y_{21}}{Y_{22}} = f\left(\frac{(a_{n21} s^{n-1} + .. + a_{021})}{s^n + .. + b_{021}}, \frac{(a_{n22} s^{n-1} + .. + a_{022})}{s^n + .. + b_{022}}\right) = -\frac{\frac{(a_{n21} s^{n-1} + .. + a_{021})}{s^n + .. + b_{021}}}{\frac{(a_{n22} s^{n-1} + .. + a_{022})}{s^n + .. + b_{022}}} \quad (17)$$

$$= \frac{f_{n-1} s^{n-1} + \ldots + f_0}{s^n + g_{n-1} s^{n-1} + .. + g_0}$$

2.6 Summary

This section summarises methods for modelling transmission lines, governed by Telegrapher's equations. Key approaches include the FDTD method for transient simulations via staggered discretization, Numerical Inverse Laplace Transform (NILT) variants (e.g., NILTcv using FFT) for frequency-to-time-domain conversion, and RLC ladder networks

RLC ladder approximations (lumped-element networks). Furthermore, AWE simplifies high-order systems via dominant poles and Pade approximations, while Y-parameters characterize admittance relationships using rational functions. In addition, complex frequency hopping is implicitly integrated via pole-residue analysis and Bromwich contour methods to enhance stability and convergence in transient simulations [9]. These methods address challenges in simulating transient and steady-state behaviours of THz lines, prioritizing trade-offs between accuracy, stability, and computational efficiency.

Chapter 3 - **Design of Transmission lines models**

3.1.1 The exact solution of Transmission lines (RLCG approach):

The exact solution of the transmission line can be derived from the RLCG ladder in the frequency domain as follows.

Writing Telegrapher equations (1) in state space

$$\frac{d}{dx}\begin{bmatrix} v(x,t) \\ i(x,t) \end{bmatrix} = \begin{bmatrix} 0 & -R(x) \\ -G(x) & 0 \end{bmatrix}\begin{bmatrix} v(x,t) \\ i(x,t) \end{bmatrix} - \begin{bmatrix} 0 & -L(x) \\ -C(x) & 0 \end{bmatrix}\frac{d}{dt}\begin{bmatrix} v(x,t) \\ i(x,t) \end{bmatrix} \quad (18)$$

Moving (18) to Laplace domain,

$$\frac{d}{dx}\begin{bmatrix} V(x,s) \\ I(x,s) \end{bmatrix} = \begin{bmatrix} 0 & -Z(x,s) \\ -Y(x,s) & 0 \end{bmatrix}\begin{bmatrix} V(x,s) \\ I(x,s) \end{bmatrix} + \begin{bmatrix} 0 & L(x) \\ C(x) & 0 \end{bmatrix}\begin{bmatrix} V(x,0) \\ I(x,0) \end{bmatrix} \quad (19)$$

Where $Z\,(x,s) = R(x) + sL(x)$, and $Y\,(x,s) = G(x) + sC\,(x)$ are series impedance. Now, let:

$$W(x,s) = \begin{bmatrix} V(x,s) \\ I(x,s) \end{bmatrix}, M = \begin{bmatrix} 0 & -Z(x,s) \\ -Y(x,s) & 0 \end{bmatrix}, and\ N = \begin{bmatrix} 0 & L(x) \\ C(x) & 0 \end{bmatrix}$$

Where

$$\frac{dW(x,s)}{dx} = M\,W(x,s) + N\,W(x,0) \quad (20)$$

Then, $W(l,s)$ at the end of the transmission line equal to,

$$W(l,s) = \Phi\,\mathrm{W}(0,\mathrm{s}) + \int_0^l e^{M(l-x)}NW(x,0)dx \quad (21)$$

Where

$$\Phi = e^{Ml}, so\ \phi = \begin{bmatrix} \Phi_{11} & \Phi_{12} \\ \Phi_{21} & \Phi_{22} \end{bmatrix} \quad (22)$$

Considering zero initial conditions ($i.e, at\ W(x,0) = 0$) then,

$$W(l,s) = \Phi\,\mathrm{W}(0,\mathrm{s}) \quad (23)$$

Or

$$W(l,s) = \begin{bmatrix} V(l,s) \\ I(l,s) \end{bmatrix} = \begin{bmatrix} \Phi_{11} & \Phi_{12} \\ \Phi_{21} & \Phi_{22} \end{bmatrix}\cdot\begin{bmatrix} V(0,s) \\ I(0,s) \end{bmatrix}$$

Considering open voltage transmission line (i.e, $I(l,s) = 0$) then,

$$\begin{bmatrix} V(l,s) \\ 0 \end{bmatrix} = \begin{bmatrix} \Phi_{11} & \Phi_{12} \\ \Phi_{21} & \Phi_{22} \end{bmatrix}\cdot\begin{bmatrix} V(0,s) \\ I(0,s) \end{bmatrix}$$

$$0 = \Phi_{21}V(0,s) + \Phi_{22}I(0,s)$$

$$I(0,s) = \Phi_{21}V(0,s) - \Phi_{22}^{-1}$$

$$V(l,s) = \Phi_{11}V(0,s) + \Phi_{12}\,I(0,s) \quad (24)$$

$$V(l,s) = \Phi_{11}V(0,s) - \Phi_{12}\,\Phi_{21}\,\Phi_{22}^{-1}V(0,s) \tag{25}$$

Re arrange (25) and simplify, the following is achieved in the s domain,

$$V(l,s) = \frac{2Vs(s)e^{l\sqrt{YZ}}}{e^{(2l\sqrt{YZ})} + 1}$$

Where $Vs(s)$ is the input in the s domain. Let,

$$x = l\sqrt{YZ}\,, \qquad so\,, V(l,s) = \frac{Vs(s)2e^{x}}{e^{(2x)} + 1}$$

Using the fact that,

$$cosh(x) = \frac{(e^{x} + e^{-x})}{2}$$

Then,

$$\frac{V(l,s)}{Vs(s)} = \frac{1}{\cosh\,(l\sqrt{YZ})} \tag{26}$$

One then can use NILTcv as in code 5, to simulate this with different values of R, L, C and G, and ultimately compare the output to the approaches mentioned earlier.

3.1.2 Exact solution using (Lumped Element Model):

In this approach, the transmission line is represented as a cascade of small segments, each consisting of a series impedance (Z series) and a parallel admittance (Y parallel) as illustrated in Figure 3.1.1. These elements correspond to the physical properties of the transmission line [10].

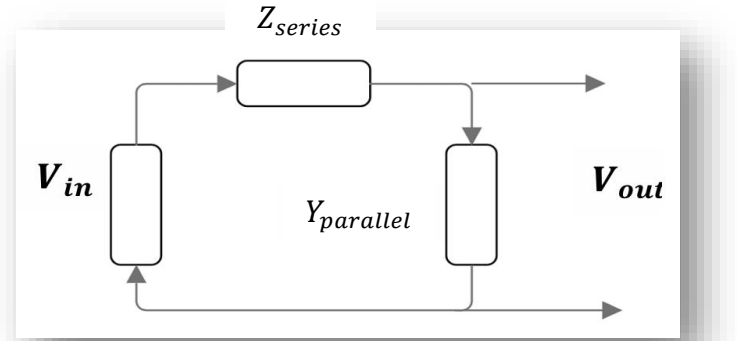

Figure 3.1.1: Equivalent circuit representation of a transmission line segment with series impedance (Z_{series}) and parallel admittance ($Y_{\{parallel\}}$).

Where,

$$Z_{series} = Z_o \sinh(\gamma l)$$

$$Z_o = \sqrt{\frac{Z}{Y}}\,, \qquad Y = G + sC, \qquad Z = (R + sL), \quad \gamma = \sqrt{ZY}$$

$$Y_{parallel} = Y_o \tanh\left(\frac{\gamma l}{2}\right), \quad Y_o = \frac{1}{Z_o} \ , \quad Z_{parallel} = \frac{1}{Y_{parallel}}$$

From Figure 4, the following equation of the transfer function is obtained:

$$T(s) = \frac{V_o}{V_{in}} = \frac{Z_{parallel}}{Z_{series} + Z_{parallel}} \tag{27}$$

$$T(s) = \frac{V_o}{V_{in}} = \frac{\dfrac{\sqrt{\dfrac{R+sC}{G+sC}}}{\tanh\left(l\dfrac{\sqrt{(R+sC)(G+sC)}}{2}\right)}}{\sqrt{\dfrac{R+sC}{G+sC}}\sinh\left(l\sqrt{(R+sC)(G+sC)}\right) + \dfrac{\sqrt{\dfrac{R+sC}{G+sC}}}{\tanh\left(l\dfrac{\sqrt{(R+sC)(G+sC)}}{2}\right)}}$$

$$T(s) = \frac{V_o}{V_{in}} = \frac{\dfrac{1}{\tanh\left(l\dfrac{\sqrt{(R+sC)(G+sC)}}{2}\right)}}{\sinh\left(l\sqrt{(R+sC)(G+sC)}\right) + \dfrac{1}{\tanh\left(l\dfrac{\sqrt{(R+sC)(G+sC)}}{2}\right)}}$$

Using the fact that,

$$\tanh\left(\frac{x}{2}\right) = \frac{\cosh(x) - 1}{\sinh(x)}$$

$$T(s) = \frac{V_o}{V_{in}} = \frac{1}{\cosh\left(l\sqrt{(R+sC)(G+sC)}\right)} \tag{28}$$

Which is the same as in (26).

3.2 AWE implementation:

AWE involves 4 main steps:

1. Form a state – space representation
2. Form the moments
3. Find the poles of the system
4. Find the residues

And then form the impulse response as:

$$h(t) = k_0\delta(t) + k_1 e^{p_1 t} + \ldots + k_n e^{p_n t} \tag{29}$$

3.2.1 Step 1: Form a state – space representation out of a model (RLC ladder or general TF):

Consider 2 sections of the RLC ladder in Figure 3, the following equations are derived:

$$v_{in} = (R_s + R_{dz})i_1 + L_{dz}\frac{di_1}{dt} + v_1 \tag{30}$$

$$v_1 = R_{dz}i_2 + L_{dz}\frac{di_2}{dt} + v_{out}$$

$$i_1 - i_2 = C\frac{dv_1}{dt}$$

$$i_2 = C\frac{dv_o}{dt}$$

Let,

$$x = \begin{bmatrix} x_1 \\ x_2 \\ x_3 \\ x_4 \end{bmatrix} = \begin{bmatrix} i_1 \\ v_1 \\ i_2 \\ v_o \end{bmatrix} \tag{31}$$

Rewriting the equations,

$$\frac{di_1}{dt} = -\frac{(R_s + R_{dz})}{L_{dz}}i_1 - \frac{v_1}{L_{dz}} + \frac{v_{in}}{L_{dz}}$$

$$\frac{di_2}{dt} = \frac{-R_{dz}i_2}{L_{dz}} - \frac{v_{out}}{L_{dz}} + v_1$$

$$\frac{dv_1}{dt} = \frac{1}{C}(i_1 - i_2)$$

$$\frac{dv_o}{dt} = \frac{1}{C}\,i_2$$

Then the state space representation is:

$$A = \begin{bmatrix} \frac{-R_s + R_{dz}}{L_{dz}} & -\frac{1}{L_{dz}} & 0 & 0 \\ \frac{1}{C} & 0 & -\frac{1}{C} & 0 \\ 0 & \frac{1}{L_{dz}} & -\frac{R_{dz}}{L_{dz}} & -\frac{1}{L_{dz}} \\ 0 & 0 & \frac{1}{C} & 0 \end{bmatrix}, B = \begin{bmatrix} \frac{1}{L_{dz}} \\ 0 \\ 0 \\ 0 \end{bmatrix}, \qquad C = [0 \quad 0 \quad 0 \quad 1] \; and \; D = 0 \tag{32}$$

If 3 sections are considered then,

$$A = \begin{bmatrix} \frac{-R_s + R_{dz}}{L_{dz}} & -\frac{1}{L_{dz}} & 0 & 0 & 0 & 0 \\ \frac{1}{C} & 0 & -\frac{1}{C} & 0 & 0 & 0 \\ 0 & \frac{1}{L_{dz}} & -\frac{R_{dz}}{L_{dz}} & -\frac{1}{L_{dz}} & 0 & 0 \\ 0 & 0 & \frac{1}{C} & 0 & -\frac{1}{C} & 0 \\ 0 & 0 & 0 & \frac{1}{L_{dz}} & -\frac{R_{dz}}{L_{dz}} & -\frac{1}{L_{dz}} \\ 0 & 0 & 0 & 0 & \frac{1}{C} & 0 \end{bmatrix}$$

In general, the RLC ladder can be expressed as state space model following the same pattern where the dimensions of matrix A is $2N$ and this is coded on MTALB in code 4, where it generates matrix A, B and C based on N.

Now, consider a general form of a transfer function that is:

$$H(s) = \frac{V_o}{V_i} = \frac{(a_{n-1}s^{n-1} + a_{n-2}s^{n-2} + \cdots + a_0)}{(s^n + b_{n-1}s^{n-1} + b_{n-2}s^{n-2} \ldots + b_0)} \tag{33}$$

This can then be converted into a state space model as follows:

$$\frac{Z(s)}{V_i} \; and \; \frac{V_o}{Z(s)}$$

$$\frac{1}{s^n + b_{n-1}s^{n-1} + .. + b_0} \xrightarrow{Z(s)} a_{n-1}s^{n-1} + a_{n-2}s^{n-2} \ldots + a_0$$

Then, converting this to time domain gives:

$$\frac{d^n z}{dt^n} + b_{n-1}\frac{d^{n-1}z}{dt^{n-1}} \ldots \ldots + b_0 Z = V_i$$

And,

$$a_{n-1}\frac{d^{n-1}z}{dt^{n-1}} + \cdots .. + a_0 Z = V_o$$

Now, let

$$x_1 = Z \, , x_2 = \frac{dz}{dt}, x_3 = \frac{d^2 z}{dt^2}, \ldots \ldots, x_{n+1} = \frac{d^n z}{dt^n} \tag{34}$$

This gives the A matrix as:

$$A = \begin{bmatrix} 0 & 1 & \dots. & 0 & 0 \\ 0 & 0 & 1 & .. & 0 \\ .. & .. & .. & .. & 1 \\ -b_0 & -b_1 & -b_2 & \dots.. & -b_{n-1} \end{bmatrix} \quad (35)$$

The B matrix:

$$B = \begin{bmatrix} 0 \\ 0 \\ \dots \\ 1 \end{bmatrix}, (nx1) entries$$

The C matrix:

$$C = [a_0 \quad a_1 \quad \dots.. \quad a_{n-1}]$$

One can make the rational fraction in (33) proper (numerator degree < denominator degree) by preforming polynomial division as follows.

$$H(s) = \frac{N(s)}{D(s)}$$

Where,

$$N(s) = Q(s)D(s) + R(s)$$

Then the proper form is:

$$H(s) = Q(s) + \frac{R(s)}{D(s)} \quad (36)$$

Where $deg(R) < deg(D)$, and the D matrix in the state space equal to $Q(s)$.

3.2.2 Step 2: Compute the moments associated with the system:

Looking at the general form of Y(s):

$$sX(s) = AX(s) + BU(s) \quad (37)$$
$$Y(s) = C^T X(s)$$

For impulse input, U(s) = 1.

$$Y(s) = C^T(sI - A)^{-1}B \quad (38)$$

If (38) is expanded about $s = 0$.

$$Y(s) = C^T(-A)^{-1}B - C^T(-A)^{-2}B(s) + C^T(-A)^{-3}Bs^2 \dots$$

But:

$$Y(s) = m_0 + m_1 s + m_2 s^2 + .. + m_n s^n \quad (39)$$

So,

$$m_0 = -C(A)^{-1}B$$
$$m_1 = Y'(s_0) = -C^T(A)^{-2}B$$
$$m_2 = \frac{Y''(s_0)}{2!} = -C^T(A)^{-3}B$$

$$m_k = \frac{Y^{(k)}(s_0)}{k!} = -C^T(A)^{-(k+1)}B \tag{40}$$

However, if $s = s_0$, then expanding (38)

$$Y(s) = C^T(s_0 I - A)^{-1}B - C^T(s_0 I - A)^{-2}B(s - s_0). + \cdots \ldots \ldots$$

So,

$$m_0 = C(s_0 I - A)^{-1}B$$

$$m_1 = Y'(s_0) = -C^T(s_0 I - A)^{-2}B$$

$$m_2 = \frac{Y''(s_0)}{2!} = C^T(s_0 I - A)^{-3}B$$

$$m_k = \frac{Y^{(k)}(s_0)}{k!} = (-1)^k C^T(s_0 I - A)^{-(k+1)}B \tag{41}$$

3.2.3 Step 3: Calculate the poles of the system

In AWE, the poles and residues are determined using the system's moments in order to obtain the time-domain model as outlined below.

Consider a general form of a transfer function.

$$H(s) = \frac{a_0 + a_1 s + a_2 s^2 + a_3 s^3}{1 + b_1 s + b_2 s^2 + b_3 s^3 + b_4 s^4} \tag{42}$$

This can be equated to: $H(s) = m_0 + m_1 s + m_2 s^2 + m_3 s^3 + \cdots$ and,

$(1 + b_1 s + b_2 s^2 + b_3 s^3 + b_4 s^4)(m_0 + m_1 s + m_2 s^2 + m_3 s^3 + \cdots) = a_0 + a_1 s + a_2 s^2 + a_3 s^3$ (16)

Multiply and equate powers of s in (16) to obtain,

$$s^0: a_0 = m_0 \tag{43}$$

$$s^1: a_1 = m_0 b_1 + m_1$$

$$s^2: a_2 = m_0 b_2 + m_1 b_1 + m_2$$

$$s^3: a_3 = m_0 b_3 + m_1 b_2 + m_2 b_1 + m_3$$

Higher powers of s:

$$s^4: 0 = m_0 b_4 + m_1 b_3 + m_2 b_2 + m_3 b_1 + m_4$$

$$s^5: 0 = m_1 b_4 + m_2 b_3 + m_3 b_2 + m_4 b_1 + m_5$$

$$s^6: 0 = m_2 b_4 + m_3 b_3 + m_4 b_2 + m_5 b_1 + m_6$$

$$s^7: 0 = m_3 b_4 + m_4 b_3 + m_5 b_2 + m_6 b_1 + m_7$$

Putting this in matrices to solve for b_i coefficients in general.

$$\begin{bmatrix} m_0 & m_1 & \ldots. & m_{q-1} \\ m_1 & m_2 & \ldots. & m_q \\ m_3 & m_4 & \ldots & .. \\ .. & \ldots & \ldots. & .. \\ m_{q-1} & \ldots & \ldots & m_{2q-1} \end{bmatrix} \begin{bmatrix} b_q \\ b_{q-1} \\ b_{q-2} \\ .. \\ b_1 \end{bmatrix} = - \begin{bmatrix} m_q \\ m_{q+1} \\ m_{q+2} \\ \ldots \\ m_{2q-1} \end{bmatrix}$$

Gaussian elimination is applied to determine the coefficients ($b_1, b_2, b_3, .., b_q$) with ($q = 4$) in this case. The poles of the system are found by solving ($B(s) = 0$). That is, solve:

$$b_q s^q + b_{q-1} s^{q-1} \ldots\ldots + b_1 s + 1 = 0 \tag{44}$$

Which gives the poles of the system.

3.2.4 Step 4: find the residues:

Generalised approach to determining the residues:

$$h(t) = \sum_{j=1}^{q} k_j e^{p_j t} \tag{45}$$

in the s domain:

$$H(s) = \sum_{j=1}^{q} \frac{k_j}{s - p_j} = \frac{a_0 + a_1 s + a_2 s^2 + \cdots + a_{q-1} s^{q-1}}{1 + b_1 s + b_2 s^2 + b_3 s^3 + \cdots + b_q s^q}$$

$$\frac{k_j}{s - p_j} = k_j \left(\frac{1}{s - p_j} \right) = -\frac{k_j}{p_j} \left(\frac{1}{1 - \frac{s}{p_j}} \right)$$

Let: $x = \frac{s}{p_j}$, Thus

$$\left(1 - \frac{s}{p_j}\right)^{-1} = 1 + \left(\frac{s}{p_j}\right) + \left(\frac{s}{p_j}\right)^2 + \left(\frac{s}{p_j}\right)^3 + \cdots \tag{46}$$

Hence:

$$H(s) = \sum_{j=1}^{q} -\frac{k_j}{p_j} \left(1 + \left(\frac{s}{p_j}\right) + \left(\frac{s}{p_j}\right)^2 + \left(\frac{s}{p_j}\right)^3 + \cdots \right) \tag{47}$$

But $H(s)$ is as in (42), then

$$m_0 = -\left(\frac{k_1}{p_1} + \frac{k_2}{p_2} + \cdots + \frac{k_q}{p_q} \right)$$

$$m_1 = -\left(\frac{k_1}{p_1^2} + \frac{k_2}{p_2^2} + \cdots + \frac{k_q}{p_q^2} \right)$$

$$m_{2q-1} = -\left(\frac{k_1}{p_1^{2q}} + \frac{k_2}{p_2^{2q}} + \cdots + \frac{k_q}{p_q^{2q}} \right)$$

Which can be solved using $V \Lambda k = -m$ where

$$V=\begin{bmatrix} 1 & 1 & \dots & 1 \\ \frac{1}{p_1} & \frac{1}{p_2} & \dots & \frac{1}{p_q} \\ \frac{1}{p_1^2} & \frac{1}{p_2^2} & .. & \frac{1}{p_q^2} \\ . & . & . & . \\ \frac{1}{p_1^{q-1}} & \frac{1}{p_2^{q-1}} & . & \frac{1}{p_q^{q-1}} \end{bmatrix}, \Lambda=\begin{bmatrix} \frac{1}{p_1} & 0 & .. & .. & 0 \\ 0 & \frac{1}{p_2} & 0 & .. & 0 \\ 0 & 0 & . & . & 0 \\ 0 & 0 & .. & \frac{1}{p_{q-1}} & 0 \\ 0 & 0 & 0 & .. & \frac{1}{p_q} \end{bmatrix}, k=\begin{bmatrix} k_1 \\ k_2 \\ . \\ . \\ k_q \end{bmatrix}, m=\begin{bmatrix} m_0 \\ m_1 \\ . \\ . \\ m_{q-1} \end{bmatrix} \quad (48)$$

Thus $k=-\Lambda^{-1}V^{-1}m$ which are the residues of the system. Finaly, the poles obtained in (44) are combined with the residues in (48) to obtain the time domain impulse response in equation (29).

3.3 Adapting AWE to Obtain a Response to a Unit Step Input (integration method):

To avoid computationally expensive explicit convolution, recursive convolution is applied based on the pole-residue representation of the transfer function [10]. For a system described in the Laplace domain as:

$$Y(s)=\frac{k_i}{s+p_i}X(s) \dots \dots \frac{d}{dt}y(t)+p_i y(t)=k_i x(t) \quad (49)$$

Assume *x*(*t*) is piecewise constant over each time interval $[t_n - t_{n-1}]$. Solving the above over the time interval using the recursive solution is:

$$y(t_n)=k_\infty x(t_n)+\sum_{i=1}^{q} y_i'(t_n) \quad (50)$$

Where

$$y_i'(t_n)=k_i\left(1-e^{p_i(t_n-t_{n-1})}\right)x(t_{n-1})+e^{-p_i(t_n-t_{n-1})}y_i'(t_{n-1}). \quad (51)$$

The equation in (51) updates the output at t_n using only the previous state $y_i'(t_{n-1})$ and the input $x(t_{n-1})$ eliminating the need to store the entire history of $x(t)$ [10].

3.4 Implementation of Y parameters:

Considering the general form derived in equation (17) with $n=2$. One can generate rational expression from a given Y values of a transmission line as follows:

$$Y_R+jY_i=\frac{a_1 s+a_0}{s^2+b_1 s+b_0} \quad (52)$$

At $s=jw$

$$(Y_R+jY_i)(-w^2+b_1 jw+b_0)=\ a_1 jw+a_0 \quad (53)$$

$$(-w^2Y_R + b_1jwY_R + b_0Y_R - w^2jY_i - b_1wY_i + jb_0Y_i) = a_1jw + a_0$$

Re-write (53) as:

$$(b_1jwY_R + b_0Y_R - b_1wY_i + jb_0Y_i) - a_1jw - a_0 = w^2Y_R + jw^2Y_i \quad (54)$$

To find the coefficients the following is applied:

$$A = \begin{bmatrix} -1 & Y_R^1 & 0 & -Y_i^1 w \\ 0 & Y_i^1 & -jw^1 & jwY_R^1 \\ \dots & \dots & \dots & \dots \\ -1 & Y_R^N & 0 & -Y_i^N w \\ 0 & Y_i^N & -jw^N & -w^2 Y_i^N \end{bmatrix}, B = \begin{bmatrix} a_0 \\ b_0 \\ a_1 \\ b_1 \end{bmatrix} \text{ and } C = \begin{bmatrix} Y_R^1 w^2 \\ jY_i^1 w^2 \\ \dots \\ Y_R^N w^2 \\ jY_i^N w^2 \end{bmatrix} \quad (55)$$

$where\ A\ B = C\ and\ B = A^{-1}B.$

Once the rational fraction is derived, AWE is used to obtain the response of the transmission line and compare it to the exact results.

(next few weeks) this will depend on what's achieved.

Filter the given Y values based on the frequency and smoothness, so the first model has points at low frequencies and combine it with the smaller models at high frequencies.

The approach to obtain an efficient model is as follows:

consider 2 models of Y parameters with 100 points of given Y values and follow the same steps for as many Y models.

1. $Y_1 = generated\ from\ the\ first\ 50\ pints.$
2. $evaluate\ Y_1 at\ the\ last\ 50\ points\ (w_1).$
3. $subtract\ the\ obtain\ values\ from\ the\ exact\ given\ value\ at\ (w_1)\ (i.e, Y_1(w_1) - exact(w_1).$
4. $use\ the\ results\ to\ obtain\ Y_2\ and\ so\ on.$

Once the model obtained and most factors affecting it are considered, it can be compared to other methods in term of accuracy and speed.

3.5 Complex frequency hopping:

Chapter 4 – Testing, Results and Discussion

This chapter evaluates the accuracy and efficiency of FDTD, RLC ladder networks and AWE with rational expression models in transmission line analysis, comparing them to exact solutions. Using root mean squared (RMS) error and computational speed as metrics (tic toc on MATLAB), the chapter highlights trade-offs between precision and resource demands. Challenges in transient response, AWE's unit step performance, and enhancements via Complex Frequency Hopping (CFH) are explored. The chapter concludes with a comparison and guiding method selection for high-speed circuit design based on accuracy and computational cost.

4.1 FDTD

Code 1 from the appendix is used with the same parameters for all methods and a load of 100 ohms. The following table and figure highlight the main results.

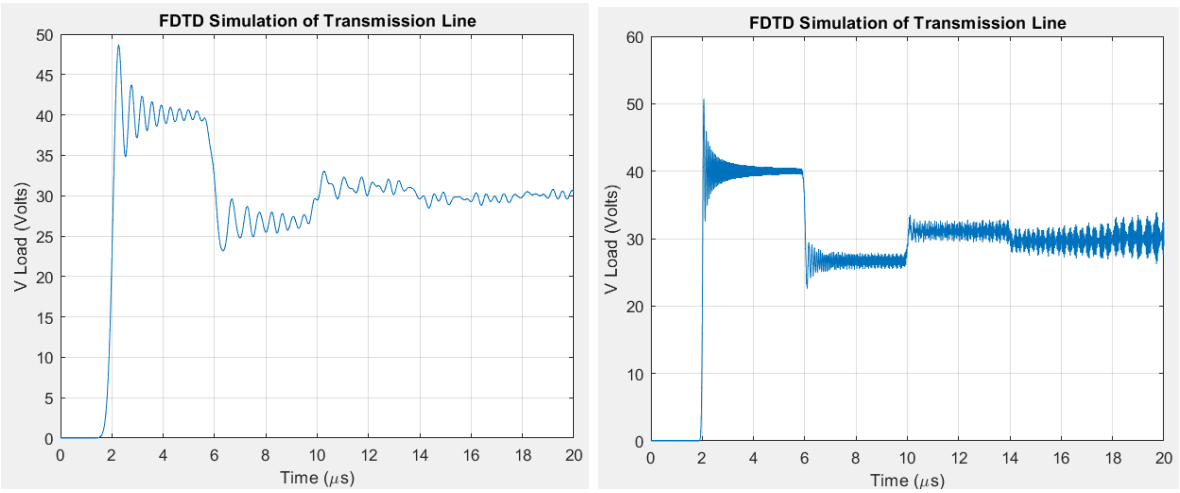

Figure 4.1.1: FDTD simulation of a transmission line with a 100 Ω load. The left plot corresponds to a discretization of 20 sections, while the right plot uses 200 sections.

Number of sections	Time taken
20	0.372277
100	1.440476
200	2.862272

The Finite-Difference Time-Domain (FDTD) method demonstrates a clear trade-off between accuracy and computational efficiency. As the number of sections increases, the time required for computation grows significantly. For instance, at 200 sections, the time taken is approximately 2.86 seconds, which is much higher compared to the RLC ladder network. The

requirement of a very small-time step to maintain accuracy further adds to its computational burden, making it less efficient for large-scale simulations.

4.2 RLC ladder

Code 2 from the appendix is used with the same parameters as in FDTD. The following table and figure show the key results.

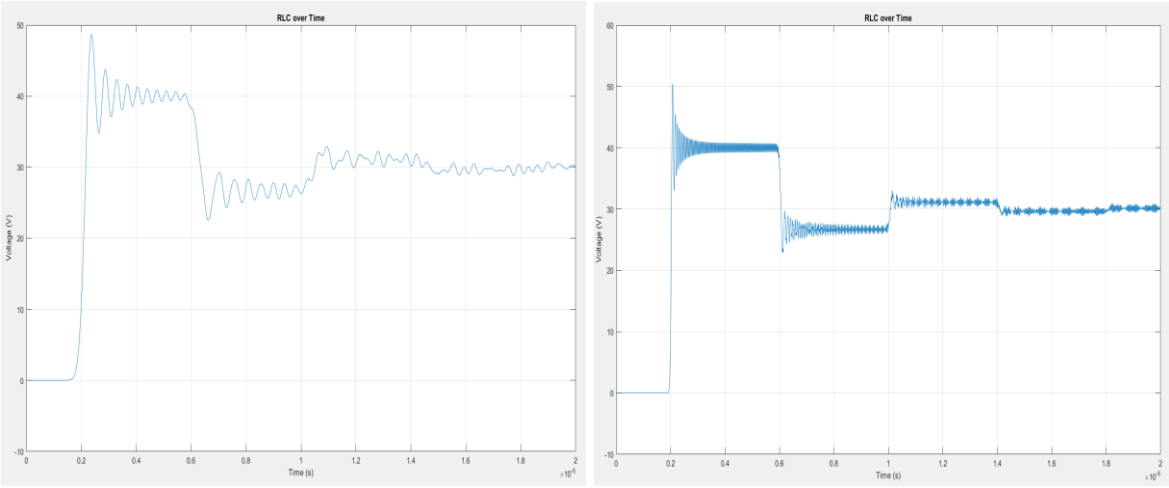

Figure 4.2.1: Voltage response of an RLC circuit over time using different discretization levels. The left plot corresponds to 20 sections, while the right plot uses 200 sections.

Number of sections	Time taken
20	0.061710
100	0.077910
200	0.127065

The RLC ladder network, particularly when solved using ode45, shows significantly better computational efficiency compared to FDTD. The results show that even with increasing sections, the time taken remains relatively low (0.127 seconds for 200 sections). This efficiency is due to the variable time step approach of ode45, which adapts to the system's behaviour dynamically, reducing unnecessary computations. The fixed time step analysis also shows that RLC performs better in terms of both accuracy and speed when compared to FDTD.

4.3 Exact solution compared with FDTD, RLC and challenges.

4.3.1 Exact solution:

The exact transmission line model for an open-circuit design is derived using equation (26) or (28). By assuming a lossless line and applying the same parameters as those used in the RLC and FDTD methods, the following results are obtained using code 6 in the appendix. These results are then compared against other models to evaluate their accuracy and computational performance.

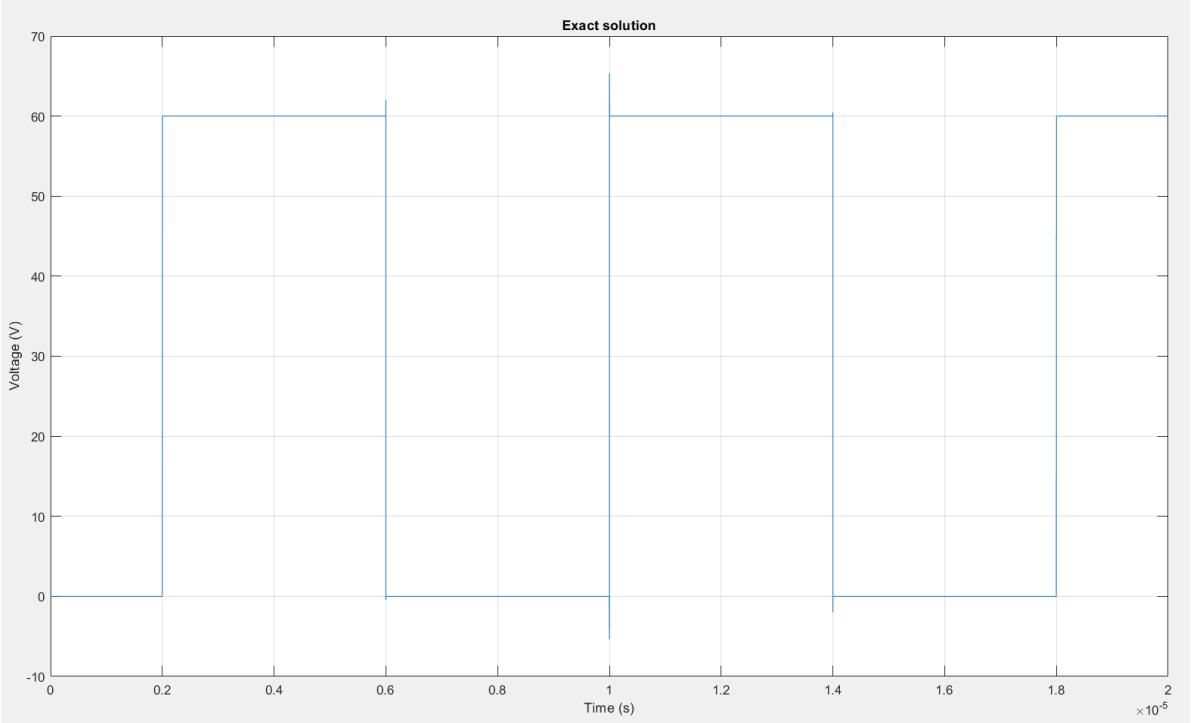

Figure 4.3.1: Simulation of the exact solution of a lossless transmission line with an open-circuit termination and a 30V input.

The result in Figure 4.3.1 is expected since the input voltage is 30V, and the transmission line is open-circuited, meaning there is no load. As a result, the wave propagates forward and then reflects backward, leading to a superposition of the incident and reflected waves. This interaction creates a square-like waveform with a peak voltage of 60V, given by $V = V^+ + V^-$.

4.3.2 RLC and FDTD

A fixed time step of $1x10^{-10}$ seconds is used for the RLC method. The table below compares the efficiency of the Finite-Difference Time-Domain (FDTD) method and the RLC ladder network in terms of Root Mean Square Error (RMSE) and computation time.

Number of sections	RLC ladder		FDTD	
	Error (RMSE)	time	Error (RMSE)	time
50	9.8279	0.497539	7.2862	0.6940
100	7.3491	0.615154	5.5268	1.277740
200	5.5411	0.923801	5.0746	2.526845
400	4.2304	1.492597	4.3942	16.828843

When a fixed time step of $1e-10$ is used for the RLC method, the results show that it consistently outperforms FDTD in terms of speed while maintaining comparable accuracy. For example, at 400 sections, RLC completes in 1.49 seconds, whereas FDTD takes a significantly longer 16.83 seconds. The root mean squared error (RMSE) values indicate that FDTD achieves slightly better accuracy in some cases (e.g., 5.0746 for 200 sections vs. 5.5411 for RLC), but the trade-off in computation time makes RLC the more practical choice. Additionally, since RLC does not rely on a small-time step, it can be scaled efficiently for higher accuracy.

4.3.3 Visual inspections of all solutions (methods)

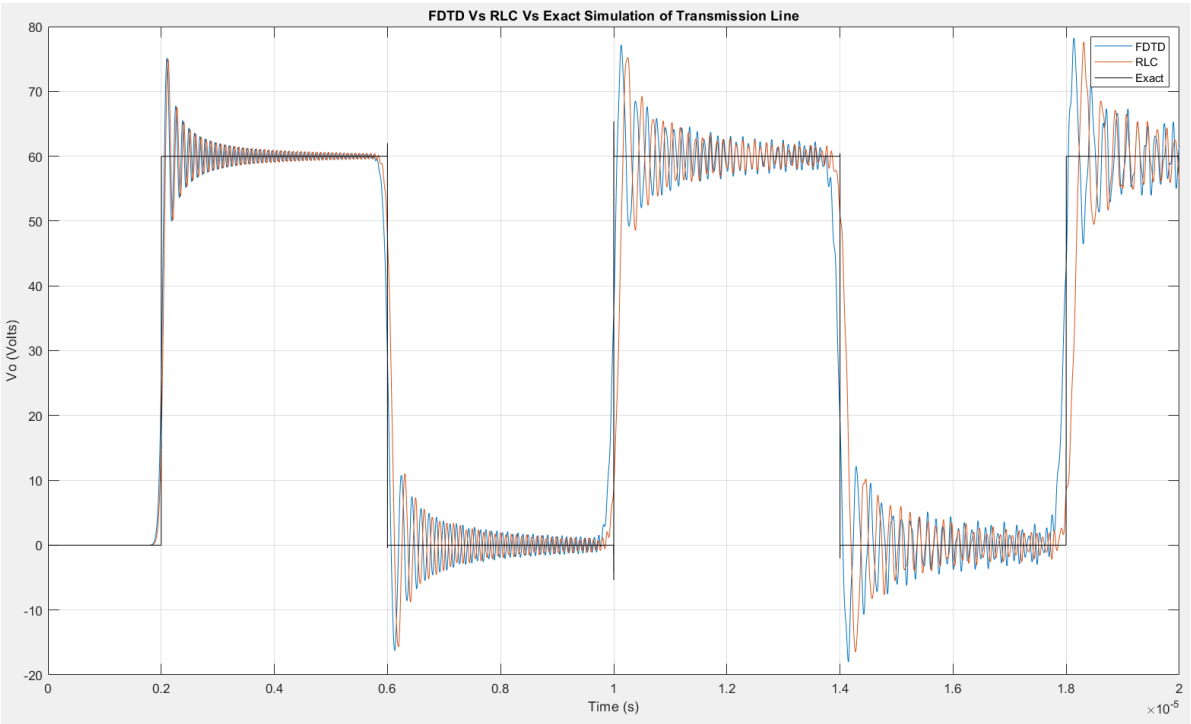

Figure 4.3.2: Comparison of FDTD, RLC ladder, and exact simulation of a transmission line, showing output voltage Vo over time with numerical oscillations.

4.4 AWE testing

4.4.1 Impulse response:

Consider the following example:

$$A = \begin{bmatrix} -2 & 1 & 0 & 0 \\ 1 & -2 & 1 & 0 \\ 0 & 1 & -2 & 1 \\ 0 & 0 & 1 & -1 \end{bmatrix}, B = \begin{bmatrix} 1 \\ 0 \\ 0 \\ 0 \end{bmatrix} \; and \; C = \begin{bmatrix} 1 \\ 0 \\ 0 \\ 0 \end{bmatrix} \tag{56}$$

One can find the impulse response by calculation moments, poles and residues using equations (40), (44) and (48) respectively,

$$m_0 = 1\,, m_1 = -4, m_2 = 30, m_3 = -246, m_4 = 2037, m_5 = -16886, m_6 = 140000$$

$$p_1 = -3.53, p_2 = -2.35, p_3 = -1, p_4 = -0.12$$

$$k_1 = 0.18, k_2 = 0.43, k_3 = 0.33, k_4 = 0.05$$

Then the impulse response is:

$$H(s) = \; 0.18e^{-3.53t} \; + \; 0.43e^{-2.35t} + 0.33e^{-t} + \; 0.05e^{-0.12t} \tag{57}$$

4.4.2 A theoretical method for validating AWE.

The impulse response of a state space model is given by:

$$y(t) = Ce^{at}B \tag{58}$$

$$where, \quad e^{at} = Me^{\Omega t}M^{-1}$$

$$and \; \Omega = M^{-1}AM = \begin{bmatrix} \lambda_1 & 0 & 0 \\ \dots & \lambda_2 & 0 \\ 0 & \dots. & \lambda_n \end{bmatrix}$$

Considering the same example with $t = 0{:}\,2$ with time step of 0.001 the following is obtained:

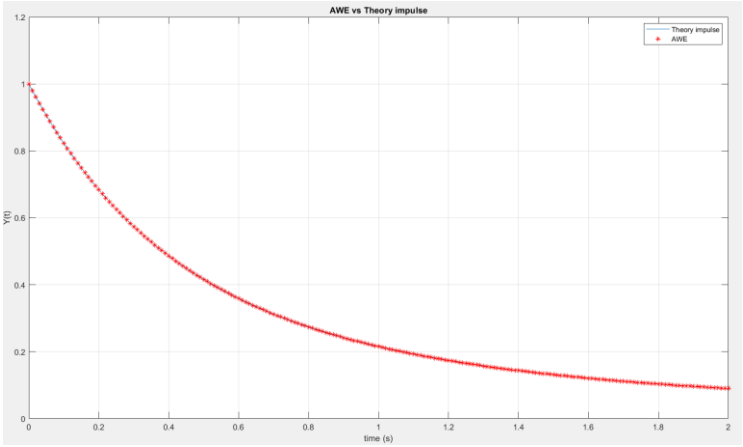

Figure 4.4.2: Comparison of AWE approximation and theoretical impulse response, showing close agreement over time.

The Asymptotic Waveform Evaluation (AWE) method is tested using a system matrix approach, generating moments, poles, and residues to derive the impulse response function. The obtained RMSE value of 5.6523e-08 indicates high accuracy, suggesting that AWE is a highly reliable method for transmission line analysis.

4.4.3-Unit step response.

Using the same example in (56),

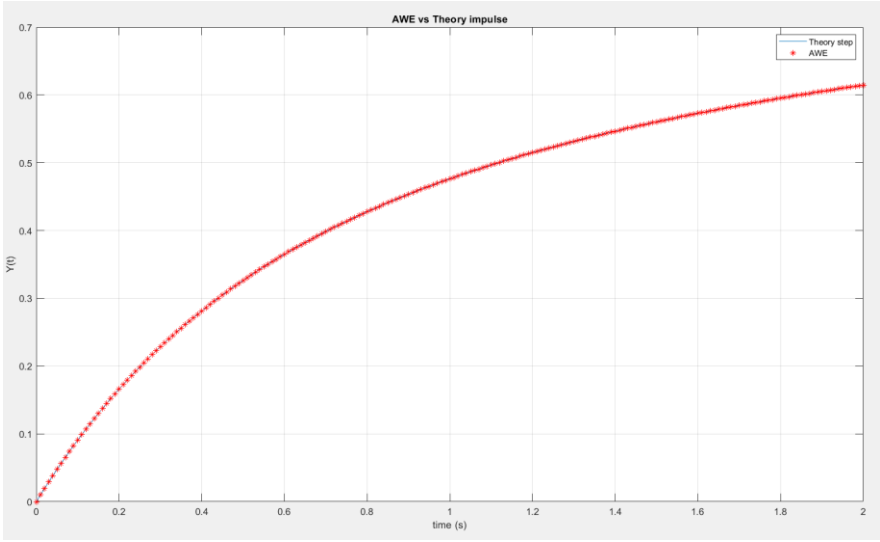

Figure 4.4.3: Comparison of AWE and the theoretical step response over time shows that AWE closely aligns with the theoretical model, highlighting its accuracy.

Similar to its impulse response, the unit step response of AWE also demonstrates exceptional accuracy, with an RMSE of 1.2973e-08. The results highlight that reducing the time step further enhances AWE's accuracy, though at the cost of increased computational time.

4.5 Generating rational expression testing.

(next few weeks) this will depend on what's achieved.

4.6 Generating transmission line testing (considering different factors).

(next few weeks) this will depend on what's achieved.

- **Comparing all methods in terms of accuracy and speed.**
- **Applying complex frequency hopping.**

Chapter 6 – Ethics

Engineering ethics play a crucial role in the responsible development and implementation of technology. This project, which focuses on the simulation and exploration of terahertz (THz) transmission lines, adheres the ethical principles outlined in the IEEE Code of Ethics, the Engineers Ireland (IEI) Code of Ethics, and best practices in software usage, ensuring fairness, integrity, and professionalism throughout the research process.

6.1 IEEE Code of Ethics

The IEEE Code of Ethics [12] highlights the importance of integrity, safety, fairness, and professional responsibility in engineering practices. In alignment with these principles, the following ethical considerations were observed throughout this project:

- **Public Safety and Welfare:** The research was conducted with a focus on minimizing risks to public welfare, ensuring transparency in reporting findings, and considering the broader impact of THz technology.
- **Honest Representation of Results:** All data, simulations, and conclusions have been presented accurately, avoiding any misleading claims or misinterpretations.
- **Proper Credit and Acknowledgment:** Previous research, methodologies, and contributions from other professionals have been properly cited to maintain intellectual integrity.
- **Avoiding Conflicts of Interest:** The work was conducted objectively, with no external influence affecting the outcomes.

6.2 Engineers Ireland (IEI) Code of Ethics

As a professional engineering project, this work also follows the Engineers Ireland (IEI) Code of Ethics [13], which mandates professional responsibility and adherence to high ethical standards. The key IEI ethical principles applied in this project include:

- **Commitment to Public Safety and Environmental Protection:** The research was conducted responsibly, ensuring that findings contribute positively to engineering knowledge without causing harm.
- **Professional Competence and Integrity:** The project was executed within the researcher's field of expertise, with clear communication of results and limitations.
- **Fairness, Courtesy, and Good Faith:** All collaborations and academic discussions were conducted respectfully and professionally, upholding ethical engineering standards.

6.3 Use of Licensed MATLAB and Software for Implementation and Testing.

In compliance with ethical engineering practices and software licensing agreements, this project exclusively used licensed versions of MATLAB and other required software for simulation, testing, and implementation. This aligns with professional engineering standards, ensuring:

- **Legal and Ethical Software Usage:** Unauthorized or pirated software was strictly avoided, maintaining compliance with intellectual property laws.
- **Reliability and Accuracy of Results:** Using licensed software ensured that the simulations and calculations were performed using verified, up-to-date tools, minimizing errors and inaccuracies.
- **Multiple Testing for Accuracy:** The achieved results were tested multiple times using different parameter variations to ensure accuracy and reliability
- **Adherence to Industry Standards:** The project follows best practices in software implementation to ensure high-quality, reproducible research outcomes.

By adhering to these ethical principles, this project upholds professional engineering standards, ensuring responsible and ethical research in THz transmission line modeling.

Chapter 7 - Conclusions and Further Research

This project evaluated the effectiveness of numerical methods for modelling terahertz (THz) transmission lines, focusing on balancing computational efficiency and accuracy. The Finite-Difference Time-Domain (FDTD) method provided foundational insights into transient and steady-state behaviours but proved computationally intensive, with simulation times escalating to 16.83 seconds for 400 sections. In contrast, the RLC ladder network, solved using MATLAB's adaptive ode45 solver, demonstrated superior efficiency, completing 200-section simulations in 0.127 seconds while maintaining competitive accuracy (RMSE: 5.5411 vs. FDTD's 5.0746 at 200 sections). The Numerical Inverse Laplace Transform (NILT) exact solution validated both methods, confirming their alignment with theoretical expectations for lossless lines. Asymptotic Waveform Evaluation (AWE) emerged as a highly accurate technique for transient analysis, achieving RMSE values as low as 1.2973×10^{-8} for step responses, though its computational cost increased with finer time steps.

This work contributes to the advancement of THz communication systems by demonstrating that RLC ladder approximations and AWE offer practical, scalable solutions for high-frequency applications. For large-scale simulations requiring rapid results, the RLC method is optimal, while AWE excels in scenarios demanding precise transient analysis. The integration of Y-parameters and pole-residue models further enhances the reliability of these tools for designing next-generation technologies such as 6G networks and biomedical imaging systems.

This will depend on what's achieved.

References

1. A. Chahadih *et al*., "Low loss microstrip transmission-lines using cyclic olefin copolymer COC-substrate for sub-THz and THz applications," *2013 38th International Conference on Infrared, Millimeter, and Terahertz Waves (IRMMW-THz)*, Mainz, Germany, 2013, pp. 1-2, doi: 10.1109/IRMMW-THz.2013.6665702.

2. D. Veerlavenkaiah and S. Raghavan, "Determination of propagation constant using 1D-FDTD with MATLAB," *2016 International Conference on Communication Systems and Networks (ComNet)*, Thiruvananthapuram, India, 2016, pp. 61-64, doi: 10.1109/CSN.2016.7823987.

3. T. P. Montoya, "Modeling 1-D FDTD transmission line voltage sources and terminations with parallel and series RLC loads," *IEEE Antennas and Propagation Society International Symposium (IEEE Cat. No.02CH37313)*, San Antonio, TX, USA, 2002, pp. 242-245 vol.4, doi: 10.1109/APS.2002.1016969.

4. Y. Shang, H. Yu and W. Fei, "Design and Analysis of CMOS-Based Terahertz Integrated Circuits by Causal Fractional-Order RLGC Transmission Line Model," in *IEEE Journal on Emerging and Selected Topics in Circuits and Systems*, vol. 3, no. 3, pp. 355-366, Sept. 2013, doi: 10.1109/JETCAS.2013.2268948.

5. C. R. Paul, "Incorporation of terminal constraints in the FDTD analysis of transmission lines," in *IEEE Transactions on Electromagnetic Compatibility*, vol. 36, no. 2, pp. 85-91, May 1994, doi: 10.1109/15.293284.

6. E. Gad, Y. Tao and M. Nakhla, "Fast and Stable Circuit Simulation via Interpolation-Supported Numerical Inversion of the Laplace Transform," in *IEEE Transactions on Components, Packaging and Manufacturing Technology*, vol. 12, no. 1, pp. 121-130, Jan. 2022, doi: 10.1109/TCPMT.2021.3122840.

7. L. Brancik, "Matlab based time-domain simulation of multiconductor transmission line systems," *The IEEE Region 8 EUROCON 2003. Computer as a Tool.*, Ljubljana, Slovenia, 2003, pp. 464-468 vol.1, doi: 10.1109/EURCON.2003.1248066.

8. K. Perutka, Ed., *MATLAB for Engineers: Applications in Control, Electrical Engineering, IT and Robotics*. Rijeka, Croatia: InTech, 2011. Available: https://doi.org/10.5772/2468.

9. W. T. Smith and S. K. Das, "Application of asymptotic waveform evaluation for EMC analysis of electrical interconnects," *Proceedings of International Symposium on Electromagnetic Compatibility*, Atlanta, GA, USA, 1995, pp. 429-434, doi: 10.1109/ISEMC.1995.523595.

10. W. T. Beyene and J. E. Schutt-Ainé, "Efficient transient simulation of high-speed interconnects characterized by sampled data," *IEEE Transactions on Components,*

Packaging, and Manufacturing Technology—Part B, vol. 21, no. 1, pp. 105-114, Feb. 1998.

11. F. Vandrevala, "Transmission Line Model for Material Characterization using Terahertz Time-Domain Spectroscopy," *Ph.D. dissertation*, Univ. of Virginia, July 2019.
12. IEEE, "IEEE Code of Ethics," IEEE, Jun. 2020. Available: https://www.ieee.org/about/corporate/governance/p7-8.html.
13. Engineers Ireland, "Code of Ethics," Engineers Ireland, Feb. 2023. Available: https://www.engineersireland.ie.

Appendix 1

Code 1 (FDTD)

```
clear
clc
% a lossless , two-conductor line with Vs(t)=30,
% Rs = 0 R, VL(t) = 0, and RL = 100 R. The line is of
% length L = 400 m and has TJ = 2 x 10' m/s and ZC = 50 R
%%%%%%%%%%%%%%%%%%%%%%%%%%%%%%%%%%%%%%%%%%%%%%%%%%%%%%%%%%%%%%%%%%%%%%%%%%%%
L_total = 400;  % Total length of the line (m)
Zc = 50;  % Characteristic impedance (Ohms)
v = 2e8;  % Speed of propagation (m/s)
Rs = 0;  % Source resistance (Ohms)
RL = 100;  % Load resistance (Ohms)
Vs = 30;%  % Input voltage (V)
% Compute inductance and capacitance
C = 1 / (v * Zc);
L = Zc/v;
NDZ = 20;  % Number of spatial steps
dz = L_total / NDZ;  % Spatial step delta z
dt = 1e-11;  % Time step delta t
t_max = 20e-6;  % Maximum simulation time (20 as in the paper)
t_steps = round(t_max / dt);  % Number of time steps
% allocate voltage and current arrays
V = zeros(NDZ+1, t_steps);
V(1,:)=Vs*ones(1,t_steps);
I = zeros(NDZ, t_steps);
% FDTD Loop for Time Stepping
for n = 1:t_steps-1
    V(1,n+1) = V(1,n);
    for k = 1:NDZ
    if k>1
        V(k,n+1) = V(k,n) + dt/(dz *C)* (I(k-1,n) - I(k,n));  % Update voltag
        dV_k = V(k-1,n) - V(k,n);  % Voltage difference between points
        I(k-1,n+1) = I(k-1,n) + dt/(dz *L) * dV_k;
    end
    end
    V(NDZ,n+1) =V(NDZ,n)+dt*(I(NDZ-1,n)/(C*dz)-V(NDZ,n)/(RL*C*dz));
end

% Plot the results for the voltage at the load
figure(1)
plot((0:t_steps-1)*dt/1e-6, V(NDZ,:));
xlabel('Time (\mus)');
ylabel('V Load (Volts)');
title('FDTD Simulation of Transmission Line');
grid on;
```

Code 2 (RLC)

```
clear
clc
len=400;
N = 20; % Number of sections in the transmission line
dz=len/N;
L = 2.5e-7*dz;   % Inductance
C = 1e-10*dz;    % Capacitance
R = 0;       % Resistance per section
Rs = 0;       % Source resistance
Rl = 100;     % Load resistance
Vs  = 30;      % Source voltage (could be a function of time)
y0 = zeros(2 * N, 1);
tspan = [0 20e-6];
% Solve using ode45
[t, y] = ode45(@(t, y) fline(t, y, N, L, C, R, Rs, Rl, Vs), tspan, y0);
% Plot voltage at the end of the transmission line (VN)
```

```
figure(1);
plot(t, y(:,N*2));  % Plot voltage at the load (VN)
xlabel('Time (us)');
ylabel('Voltage at Load (V)');
title('RLC Voltage at Load over Time');
grid on
```

Code 3 (fline function)

```
function df = fline(t, y,N,L,C,R,Rs,Rl,Vs)
    % the use of t involves input dependent on time (i.e, sin(t))
    df = zeros(2 * N, 1);
    % Currents and voltages
    In = y(1:2:2*N);  % Currents
    Vn = y(2:2:2*N);  % Voltages
    % Boundary conditions at the source end (n=1)
    df(1) = (-1 / L) * Vn(1) - (Rs + R) / L * In(1) + (1 / L) * Vs;  % dI1/dt
    df(2) = (1 / C) * In(1) - (1 / C) * In(2);  % dV1/dt
    % Interior sections (n=2 to N-1)
    for n = 1:N-1
        df(2*n + 1) = (-1 / L) * Vn(n+1) - R / L * In(n)+(1 / L) * Vn(n);  % dIn/dt
        df(2*n) = (1 / C) * In(n) - (1 / C) * In(n+1);  % dVn/dt
    end
    df(2*N-1) = (-1 / L) * Vn(N) - R / L * In(N) + (1 / L) * Vn(N-1);
    df(2*N) = (1 / C) * In(N) - Vn(N) / (Rl * C);  % dVN/dt (voltage at the load)
end
```

Code 4 (NILTcv)

```
function [ft,t]=niltcv(F,tm,depict);
alfa=0; M=2506; P=3; Er=1e-10; % adjustable
N=2*M; qd=2*P+1; t=linspace(0,tm,M); NT=2*tm*N/(N-2);
omega=2*pi/NT;
c=alfa+log(1+1/Er)/NT; s=c-i*omega*(0:N+qd-1);
Fs(:,:,1)=feval(F,s); Fs(:,:,2)=feval(F,conj(s)); lv=size(Fs,1);
ft(:,:,1)=fft(Fs(:,:,1),N,2); ft(:,:,2)=N*ifft(Fs(:,:,2),N,2);
ft=ft(:,1:M,:);
D=zeros(lv,qd,2); E=D; Q=Fs(:,N+2:N+qd,:)./Fs(:,N+1:N+qd-1,:);
D(:,1,:)=Fs(:,N+1,:); D(:,2,:)=-Q(:,1,:);
for r=2:2:qd-1
 w=qd-r;
 E(:,1:w,:)=Q(:,2:w+1,:)-Q(:,1:w,:)+E(:,2:w+1,:);
 D(:,r+1,:)=-E(:,1,:);
 if r>2
 Q(:,1:w-1,:)=Q(:,2:w,:).*E(:,2:w,:)./E(:,1:w-1,:);
 D(:,r,:)=-Q(:,1,:);
 end
end
A2=zeros(lv,M,2); B2=ones(lv,M,2); A1=repmat(D(:,1,:),[1,M,1]);
B1=B2; z1=repmat(exp(-i*omega*t),[lv,1]); z=cat(3,z1,conj(z1));
for n=2:qd
 Dn=repmat(D(:,n,:),[1,M,1]);
 A=A1+Dn.*z.*A2; B=B1+Dn.*z.*B2; A2=A1; B2=B1; A1=A; B1=B;
end
ft=ft+A./B; ft=sum(ft,3)-repmat(Fs(:,1,2),[1,M,1]);
ft=repmat(exp(c*t)/NT,[lv,1]).*ft; ft(:,1)=2*ft(:,1);
switch depict
 case 'p1', plott1(t,ft); case 'p2', plott2(t,ft);
 case 'p3', plott3(t,ft); otherwise display('Invalid Plot');
end
```

```
% --- Plotting functions called by 1D NILT, vector version ----
%----------- Multiple plotting into single figure -------------
function plott1(t,ft)
```

```
figure; plot(t,real(ft)); grid on;
%figure; plot(t,imag(ft)); grid on; % optional
%---------- Plotting into separate figures ----------------
function plott2(t,ft)
for k=1:size(ft,1)
 figure; plot(t,real(ft(k,:))); grid on;
 figure; plot(t,imag(ft(k,:))); grid on; % optional
end
% ------------------ Plotting into 3D graphs ------------------
function plott3(t,ft)
global x; % x must be global in F
 m=length(t); tgr=[1:m/64:m,m]; % 65 time points chosen
 figure; mesh(t(tgr),x,real(ft(:,tgr)));
 figure; mesh(t(tgr),x,imag(ft(:,tgr)));
```

Code 5 (Exact solution with NILTcv)

```
clear
clc
R = 0;        % Resistance per unit length (Ohms per meter)
L = 2.5e-7;     % Inductance per unit length (Henries per meter)
G = 0;        % Conductance per unit length (Siemens per meter)
C = 1e-10;    % Capacitance per unit length (Farads per meter)
l = 400;    % Length of the transmission line (meters)
vs = 30;
t= 0:1e-11:20e-6;
h = t(2) - t(1);
% Calculate propagation constant (gamma) in the s-domain
z = @(s)(R+s.*L);
y = @(s)(G + s .* C);
gamma = @(s)sqrt(z(s) .* y(s));
% Calculate characteristic impedance (Z0) in the s-domain
Z0 = @(s) sqrt(z(s) ./ y(s));
% Calculate series impedance (Z_series) in the s-domain
Z_series =@(s) Z0(s) .* sinh(gamma(s) .* l);
Y_parallel =@(s) (1 ./ Z0(s)) .* tanh((gamma(s) .* l)./2); %y *tanh(gamma*l/2)
% Calculate parallel impedance (Z_parallel) in the s-domain
%Z_parallel =@(s) Z0(s) ./ tanh(gamma(s) .* l);
Z_parallel = @(s) 1./Y_parallel(s);
% Transfer function TF = Z_parallel / (Z_series + Z_parallel)
TF = @(s) Z_parallel(s) ./ (Z_series(s) + Z_parallel(s));
vo = @(s) TF(s) * vs./s;
%simplified
%vo = @(s) vs./(s.*cosh(l.*(G + C.*s).^(1/2).*(R + L.*s).^(1/2))); %
[y,t]=niltcv(vo,20e-6,'p1');
```

Code 6 (RLC to state space)

```
clear
clc
Rs =0;
Rdz = 5;
Ldz = 2;
Cdz =10;
N = 4;
numStates = 2 * N; % Each section has 2 states (current and voltage)
A = zeros(numStates, numStates);% Initialize A matrix
for i = 1:N
    if i == 1
        A(1, 1) = -(Rs + Rdz) / Ldz; % firs term (Rs + Rdz)
    else
        A(2*i-1, 2*i-1) = -Rdz / Ldz;
    end
    if i > 1
        A(2*i-1, 2*(i-1)) = 1 / Ldz;
```

```
        A(2*i-1, 2*i) = -1 / Ldz;
    end
    if i < N
        A(2*i-1, 2*i) = -1 / Ldz;
        A(2*i, 2*i-1) = 1 / Cdz;
        A(2*i, 2*i+1) = -1 / Cdz;
    else
        A(2*i, 2*i-1) = 1 / Cdz;
    end
end
% Initialize B matrix
B = zeros(numStates, 1);
B(1) = 1 / Ldz;
%C matrix
C = zeros(1, numStates);
C(end) = 1;
```

Code 7 (AWE s=0)

```
function [h_impulse,h_s, y_step, t] = AWE(A,B,C,D,input,time)
    t = linspace(0,time,250);
    q = length(B);
    num_moments = 2 * q;
    moments = zeros(1, num_moments);
    [r,c]=size(C); % make sure C matrix in correct form
    if r~=1
        C= C';
    end
    for k = 1:num_moments
        moments(k) = (-1) * C * (A)^-(k) * B;
    end
    moments(1)=moments(1)+D;
    approx_order = length(B);

    % Construct the moment matrix
    moment_matrix = zeros(approx_order);
    Vector_c = -moments(approx_order+1:2*approx_order)';

    for i = 1:approx_order
        moment_matrix(i, :) = moments(i:i+approx_order-1);
    end

    % Solve for denominator coefficients
    b_matrix = moment_matrix^-1 * Vector_c;

    % Compute poles
    poles = roots([b_matrix', 1]);

    % Compute residues
    V = zeros(approx_order);
    for i = 1:approx_order
        for j = 1:approx_order
            V(i, j) = 1 / poles(j)^(i-1);
        end
    end

    A_diag = diag(1 ./ poles);
    r_moments = moments(1:approx_order);
    residues = -1 * (A_diag \ (V \ r_moments'));

    % Impulse response
    h_impulse = zeros(size(t));
    for i = 1:approx_order
        h_impulse = h_impulse + residues(i) * exp(poles(i) * t);
    end
    h_s =@(s) 0;
    for i = 1:length(poles)
        h_s =@(s) h_s(s) + residues(i)./(s-poles(i));
```

```
    end

    % Step response using recursive convolution
    y_step = zeros(size(t));
    y = zeros(length(poles), 1);

    for n = 2:length(t)
        dt = t(n) - t(n-1);
        exp_term = exp(poles * dt);
        for i = 1:length(poles)
            y(i) = residues(i) * (1 - exp_term(i))/(-poles(i)) * input + exp_term(i) * y(i);
        end
        y_step(n) = sum(y);
    end
end
```

Code 8 (generate Y parameters (rational approximation))

```
function [H_impulse,num,deno]=generate_yp2(realV,imagV,wo)
Yr = realV;  % Real part of Y11
Yi = imagV; % Imaginary part of Y11
w = wo;
A = [];
C = [];
% Loop through each frequency point to construct A and C
A = [];
C = [];
% Loop through each frequency point to construct A and C
for k = 1:length(w)
    wk = w(k);
    Yr_k = Yr(k);
    Yi_k = Yi(k);
    % Construct rows for A and C
    A_row1 = [-1, Yr_k, 0, -wk*Yi_k]; % Real part
    A_row2 = [0, Yi_k, -wk, wk*Yr_k]; % Imaginary part

    % Append to A
    A = [A; A_row1; A_row2];
    % C
    C_row1 = wk^2 * Yr_k; % Real part
    C_row2 = wk^2 * Yi_k; % Imaginary part
    % Append to C
    C = [C; C_row1; C_row2];
end

% Solve for B = [a0; b0; a1; b1]
B = A \ C;
% get cof
a0 = B(1);
b0 = B(2);
a1 = B(3);
b1 = B(4);
num = [a1,a0];
deno = [1,b1,b0];
% generated H
H_impulse =@(s) (a1*s+a0)./(s.^2+b1*s+b0);
end
```

Code 9 (Generate state space model)

```
function [A,B,C,D]= create_state_space(nem,deno)
N = nem;
D = deno;
% Perform polynomial division to make it strictly proper
[Q, R] = deconv(N, D);
% check leading coefficient (assumed to be 1)
```

```
if D(1) ~= 1
    D=D/D(1);
    N = N/D(1);
    [Q, R] = deconv(N, D);
end
% Extract coefficients for state-space representation
g = D(2:end);  % Exclude leading coefficient ( g terms )
% f terms
if R(1) ==0
    f=R(2:end);
else
    f = R;
end
% Construct state-space matrices
n = length(g); % Order of system
A = [zeros(n-1,1), eye(n-1); -flip(g)];
B = [zeros(n-1,1); 1];
C = flip(f);
D = Q;
end
```